Aerodynamic Induction System for a High-Performance Racecar

Design, Build, Test Cycle 2: Final Report

Clark Zhang, Ella Escobar, Philmon Gashaw, Santino Clemente

Table of Contents:

1. Introduction....3
1.1 Rules and Design Constraints....4
1.2 Component Overview....5
1.2.1 Air Filter....5
1.2.2 Throttle....5
1.2.3 Venturi....6
1.2.4 Plenum....8
1.2.5 Runner....8
2. Methodology....9
3. Complete Design....10
3.1 Component Design....11
3.1.1 Air Filter....11
3.1.2 Throttle....11
3.1.3 Venturi....14
3.1.4 Plenum....17
3.1.5 Runner....18
3.1.6 Gaskets, and Hardware....19
3.2 Analysis of Complete Design....21
3.3 DBT 2 Outcomes....22
4. Next Steps and Lessons Learned....22
5. Conclusions....23
6. Engineering Design Considerations....24
7. Appendix....25

Figure 1. (Left) Vanderbilt Motorsports VUM-24 vehicle during the Endurance event. (Right) Baseline intake system, used during the Formula SAE 2023-2024 season.

1. Introduction

The Vanderbilt Motorsports 2025 Formula SAE vehicle is a single-seater, open-wheeled vehicle optimized for short-course, autocross-style tracks. The powertrain for the vehicle consists of the intake, engine, exhaust, transmission, differential and drive shafts. The goal of this project is to design, build, and test a high-performance intake system that will replace the baseline system for the Vanderbilt Motorsports 2025 Formula SAE vehicle. For the scope of this project (ME 4950), only the intake system is undergoing major changes, while modifications to the engine, exhaust, and other powertrain systems fall under Next Steps, in **Section 4.**

The complete intake system for a naturally aspirated Formula SAE car typically consists of five main components, shown in Figure 1 and discussed in detail in **Section 1.2**, which come together to meet three main goals:

1. Maximize air flow into the engine
2. Increase responsiveness to throttle inputs
3. Be robust while minimizing weight

A Yamaha YFZ450 engine is used for Vanderbilt Motorsports Formula 2025 SAE vehicle. It is a single-cylinder engine, bored out for a displacement of 501 cubic centimeters (cc), with a pair of valves each for the intake and exhaust ports. As the engine completes the exhaust stroke of its four-stroke cycle and the piston reaches the top-dead-center (TDC) position, the intake valves open, drawing an air-fuel mixture into the combustion chamber as the piston moves to the bottom-dead-center (BDC) position. The intake valves close at BDC, and the inertia stored in the engine (crankshaft, counterweight) and powertrain (wheels, transmission) is converted into kinetic energy, compressing the air-fuel mixture to TDC. Near TDC, the spark plug fires, combusting the gas, forcing the piston down to BDC and starting the exhaust stroke. Once the engine is running, this combustion cycle happens several thousand times per minute (for one

combustion cycle, the crankshaft rotates two times, which is measured as revolutions per minute or RPMs), demanding 501 cc of air to enter the engine hundreds of times per second.

The chemical potential energy flow rate into the engine is determined by the fuel flow rate. There must be a sufficient amount of air for the fuel to mix with to meet the stoichiometric maximum power output. For gasoline engines, this value is known as the Air-Fuel Ratio, stoichiometrically 14.7 grams of air per 1 gram of fuel (Hillier and Pittuck 1972). In a naturally aspirated system, there is a limit to the amount of air that can be in the engine imposed by the volume of the engine. The faster that air can be pulled through the intake system into the engine, the closer that the amount of air in the engine reaches this limit. The difference between the air pressure in the engine and air pressure in the intake system is known as the volumetric efficiency. Higher volumetric efficiency leads to an increase in engine power and torque. This increase in performance can be directly measured on a dynamometer, which is discussed in **Section 2**.

The air flow rate is controlled by the throttle. Changes in the throttle angle directly affect the atmospheric conditions within the intake system. Ideally, the conditions change instantaneously in response to driver inputs; realistically, there is a short lag between the two. By optimizing the shape and volume of the intake system, this lag can be tuned and minimized, increasing the responsiveness of the powertrain.

The entire intake system undergoes many loading cycles as the pressure within the intake system changes throughout the length of a racetrack. Furthermore, there are vibrational loads that are imparted from the suspension, through the chassis, and into the intake system. Rocks and other Foreign Object Debris (FOD) should not be permitted to enter the intake system (and potentially ruin the engine), nor should it cause any jams in the moving components on the intake. The entire system should be designed to withstand the dynamic loads imparted onto it, and be resistant to FOD and other environmental variables (sun, rain, fuel, chemicals).

1.1 Rules and Design Constraints

The rules that govern the design of the intake system for a Internal Combustion (IC) Formula SAE vehicle are outlined in Sections IC.1 to IC.3 of the Formula SAE 2025 Rules (SAE International 2024, 80-84). The most important rules pertaining to the overall design of the intake are listed below:

IC.2.4.2 The only allowed sequence of components is:
- a. For naturally aspirated engines, the sequence must be: throttle body, restrictor, and engine.

IC.2.4.3 The maximum restrictor diameters at any time during the competition are:
- a. Gasoline fueled vehicles 20.0 mm

These requirements are imposed to limit the power output of Formula SAE vehicles, and keep track speeds to a manageable level for college students.

1.2 Component Overview

1.2.1 Air Filter

The air filter is a critical component of the intake system, responsible for preventing contaminants such as dust and debris from entering the engine. The Formula SAE 2025 Rules don't have any specific requirements regarding the usage and implementation of an air filter, giving teams full freedom to select, design, and integrate air filters for the unique requirements of their intake systems.

Most Formula SAE teams, including Vanderbilt Motorsports, utilize commercial off-the-shelf air filters because they are reliable, high-performing, and relatively cheap. Vanderbilt uses an ITG Maxogen JC62 air filter (see Figure A1), which was selected for its proven performance and compatibility with intake system requirements. Although different commercial air filters will be considered in the future to further optimize the design, the JC62 will initially be reused in the new intake design to enable an accurate comparison of performance metrics.

While the air filter itself is standardized, the design of the housing that holds the filter plays a role in optimizing system performance. The housing shape directly impacts how air flows into the throttle body and through the venturi, influencing aerodynamic efficiency and the air-fuel mixture delivered to the engine. An improperly designed housing can introduce turbulence or flow separation, reducing the efficiency of the entire intake system.

1.2.2 Throttle

The throttle varies the amount of air that can enter the intake system, and changes the pressure inside the intake system. Section IC.3.1 outlines the throttle design constraints:

IC.3.1.1 The vehicle must have a carburetor or throttle body.
- a. The carburetor or throttle body may be of any size or design.

IC.3.2 The throttle may be operated
- a. Mechanically by a cable or rod system

IC.3.3.1 The throttle cable or rod must:
- a. Have smooth operation
- b. Have no possibility of binding or sticking

IC.3.3.2 The throttle actuation system must use two or more return springs located at the throttle body.

In race cars, the two main types of throttles are butterfly throttles and barrel throttles, pictured in Figure A1. The butterfly consists of a flat plate, typically oval in shape, that rotates inside a cylindrical cavity. The plate is connected to an axle, which is actuated by the mechanical throttle cable. As the plate rotates, the cross-sectional area changes. However, at wide open throttle (WOT), the plate takes up a small amount of area inside the throttle, which could reduce performance at higher throttle angles. The barrel throttle attempts to solve this problem by replacing the flat plate with two counter-rotating cylinders. The two cylinders both have a cutout, allowing for air to pass unimpeded through the throttle at WOT. Barrel throttles are typically regarded as being bulkier and more complex to build due to the counter-rotating mechanism, and greater rotational inertia of the barrels.

Both throttles have non-linear relationships between cross-sectional area and throttle position. This is reflected in the flow curves for the throttles, which relate mass air flow and throttle position. As a result, the cable cam that converts the linear mechanical motion from the pull cable to the rotational motion of the throttle can be designed to change the motion ratio throughout the range of travel, adjusting the effective flow curve for the throttle.

The throttle actuation method must be designed so it cannot bind or stick at any throttle position. Low-friction bearing surfaces or ball bearings are typically used to support the rotating components in the throttle. The two return springs are used to bias the throttle to the idle position when the accelerator pedal is unpressed. A stuck throttle could spell disaster for a vehicle on the racetrack as the driver cannot control the engine's speed, aside from using the brake pedal. This exact scenario happened to Vanderbilt during the 2024 Formula SAE Michigan competition; the entire throttle body rotated about the venturi upon which it was pressed into, causing the throttle to be stuck wide open for the duration of an autocross event. Narrowly avoiding catastrophe, the team is self-imposing a requirement that throttle designs must have positive locking mechanisms and shielding that prevent the cable from being jammed.

Some teams use Electronic Throttle Control (ETC), rather than using a mechanical cable to actuate the throttle. In this configuration, changes in accelerator pedal position are measured and sent to the Electronic Control Unit (ECU), which will perform calculations and send a signal to the ETC to rotate the throttle. Designing an ETC can allow for greater control over the throttle position, and correct for non-linearity in the throttle area curves, at the cost of complexity.

1.2.3 Venturi

The 20 mm restriction is the most important component for the intake system; optimally, the mass flow rate through the restriction should be the limiting factor in the intake system. This restriction limits the engine's power, so improving this section will optimize flow to the entire system. The venturi effect is the drop in the static pressure of a fluid through a constricted ara of a pipe, flowing at subsonic speeds. The intake system benefits from this effect when implemented because it allows the air to move through the restriction much quicker and more efficiently.

The design considerations for the venturi are the length and angle of the converging and diverging sections, inlet and outlet diameter, shape, and pressure differences. Optimizing these sections is imperative for the maximum amount of air to be in the plenum at all times, so the engine has immediate access to a large volume of air upon changing engine needs. Our two baseline tests will be the venturi design on the current intake model and the maximum mass flow rate during choke flow, which is 0.0703kg/s (Singhal and Mallika 2013).

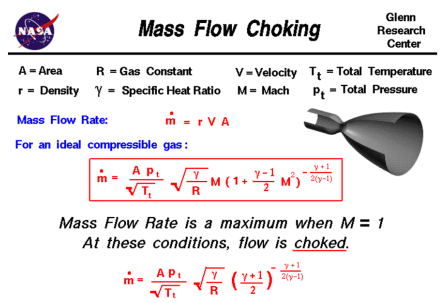

Figure 2: Mass flow choking equation from NASA when designing rocket nozzles

The current model on the Vanderbilt Motorsports Formula SAE vehicle is a 28mm Formula Student Individual Throttle Body made by AT Power, which is a combination design of the filter housing, throttle body, and venturi. The venturi is the limiting factor within this design; the behavior of the current design must be understood to move forward with a new design.

The Formula SAE Intake System Restriction results are outlined below:

1. IC.2.4.1 All airflow to the engine(s) must pass through a single circular restrictor in the intake system
2. IC. 2.4.2 The only allowed sequence of components is:
    a. For naturally aspirated engines, the sequence must be: throttle body, restrictor, and engine.
3. IC 2.4.3 The maximum restrictor diameters at any time during the competition are:
    a. Gasoline Fueled Vehicles - 20.0mm
4. IC 2.4.4 The restrictor must be located to facilitate measurement during Technical Inspection
5. IC 2.4.5 The circular restricting cross section must not be movable or flexible in any way
6. IC 2.4.6 The restrictor must not be part of the movable portion of a barrel throttle body

Our objective is to maximize the airflow through the restrictor as close to the maximum choke flow of 0.0703 kg/s as possible while abiding by the outlined rules.

Design Constraints:

Constraint:	Solution/Reason:
20mm Restriction	Venturi Design
28mm Inlet Restriction Due to throttle body	Converging Angle adjustment
Cannot exceed Sonic Flow	Causes a shock reaction that may damage intake
Vacuum Pressure cannot exceed 24.5 in Hg	If exceeded component could implode
5-15° converging and diverging angles	To satisfy the venturi effect

1.2.4 Plenum

The plenum is an aerodynamic device intended to circumvent the power limitations of the restrictor. Air that passes through the restrictor is collected in the plenum before passing into the runner. This large volume of air can be instantly accessed by the engine when needed, rather than having to draw the required air through the restrictor. This is particularly beneficial during acceleration; when the throttle angle is increased, the ECU is commanded to inject more fuel, increasing the engine power and RPMs. This increases the air flow rate required to stoichiometrically combust the fuel, which the plenum can help supply. However, as plenum volume increases, more lag is introduced into the system because the engine must cycle through all the air in the plenum before new atmospheric conditions can arise.

The plenum also dampens the shockwaves emanating from the combustion chamber. The pressurized exhaust that leaves the combustion chamber during the exhaust stroke leaves behind a low pressure wake. Towards the end of the exhaust stroke, the intake valves open, creating a period of overlap between the intake and exhaust valves. The low pressure wake draws the air-fuel mixture from the intake into the combustion chamber, known as scavenging. However, the piston is still moving up at this point in time, forcing some of the exhaust back into the intake manifold, resulting in backpressure that travels up the intake manifold, known as exhaust reversion. The plenum reduces the magnitude of this shockwave, and can be used to cancel it out entirely.

Finding the right balance for plenum volume is important for tuning performance of the engine. Using a value of 1.5 times the engine volume is a good starting point for tuning the plenum volume (Speed Talk 2008).

1.2.5 Runner

The runner is the component that acts as an interface between the engine and the rest of the intake assembly. In this final component, fuel and air are mixed in preparation for combustion – the mount for a fuel injector is thus located on the runner itself.

Several parameters define the behavior of a runner, the principles of which are the diameter, length, taper angle, and interior texture of the runner. Tangent to these attributes is the angle at which the fuel injector is mounted to the runner, where the nature of the fuel-air mixture can be altered. The diameter and length of the runner both affect the flow of air through the runner, establishing clear resistive behaviors dictating the turbulence of the air. Decreasing the diameter of the runner decreases flow, as does lengthening the runner.

The length of the runner does cause certain flow restrictions, but its greater effect relates to the engine's performance at different RPM ranges. A longer runner will contribute directly to increased torque at a lower RPM, whereas a shorter runner will contribute to higher power output at higher RPM ranges.

The interior texture of the runner also plays a notable role in the performance of the component and the car. Similar to a rifled gun barrel, adding a spiralized texture to the interior of the runner will promote beneficial turbulence that aids in both maintaining the velocity of the air flowing through the runner as well as the mixture of fuel and air.

The parameters of the runner are relatively free of regulatory restricting factors, thus there is significant freedom of design that is possible through its iterations. After flow benching designs with different interior textures, lengths, and dimensioning, it was determined that an ideal first iteration runner is 70 millimeters tall with a semi-aggressive spiral profile and a modular fuel injector mount assembly that allows for interchangeability and rapid testing.

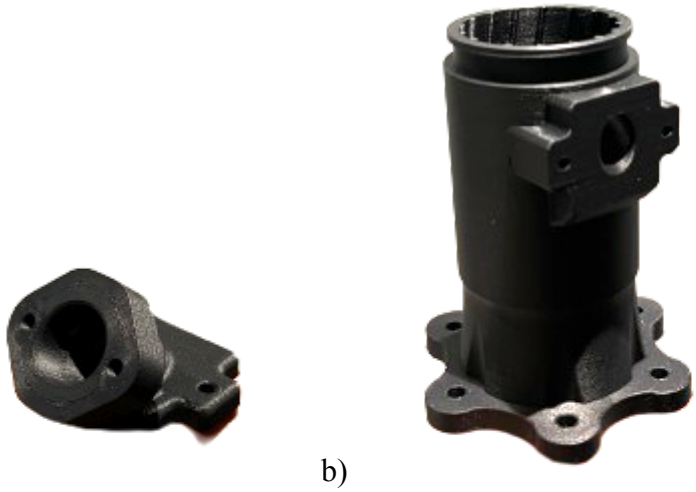

a) b)

Figure 3: a) New fuel injection design that connects to the inlet on the side of the runner
b) New runner design

2. Methodology

Computer Aided Design (CAD) software was used in the design of the intake system. Fusion 360 was chosen as the primary CAD software for its simple user interface, and previous experience from team members. SOLIDWORKS 2024 was also used for some more advanced modeling features.

The design of each component of the design was specialized to one group member and iterated on throughout the course of the semester. CAD designs were modeled for two configurations, one for flow benching and one for integration of the full-stack (all five components assembled together in a complete system). New designs were first printed in PLA at the Vanderbilt Design Studio, in the flow bench configuration for testing.

The flow bench is a tool used in the automotive industry to analyze volumetric flow rate through an orifice at different test pressures, shown in Figure A4. An intake component is placed onto the orifice plate, and the bench is turned on. The test pressure can be varied from 0 to 10 inches of water (inWg). The flow rate through the component is determined by the flow percentage manometer. Depending on the configuration of exhaust ports open at the top, the flow percentage corresponds to a volumetric flow rate shown in the chart fastened to the flow bench.

Components with higher volumetric flow flows are directly proportional to higher mass flow rates. When deciding between designs, volumetric flow rate was the primary parameter used for trading. Computational Fluid Dynamics (CFD) was also used as a secondary trade parameter. The CFD was conducted in ANSYS Fluent, and the air was modeled as turbulent flow with non-negligible surface roughness (discussed in the next section).

Once a final prototype was converged upon, the integration configuration for each component was printed from CF-ASA. This was chosen for its high tensile strength (34.3 MPa), low shrinkage, chemical resistance, UV-resistance, and water-tightness (Bambu Labs 2024). Furthermore, ASA can be smoothed with acetone. The 3D-printing process leaves behind macroscopic ridges due to the layer-by-layer deposition. Acetone smoothing melts the layer lines together due to the liquid surface tension, significantly reducing the surface roughness of the final part.

3. Complete Design

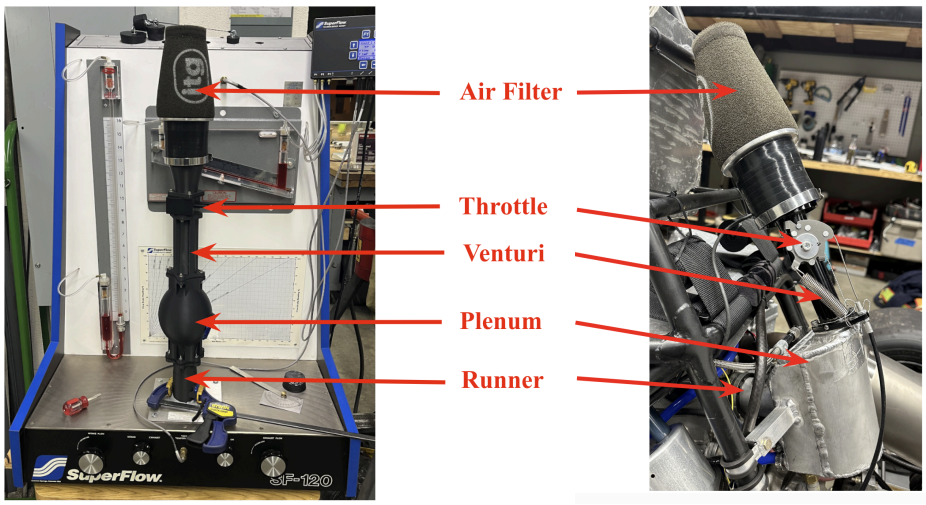

Figure 4. (Left) Full Stack, each component assembled together with gaskets, on top of the SF-120 Flow Bench. This full stack test was conducted with a placeholder PLA throttle. (Right) Baseline Intake system, used on the VUM-24 vehicle.

The greatest loads imposed on the intake system are vacuum pressures generated by the engine. The Yamaha engine creates absolute pressures within the combustion chamber ranging from atmospheric pressure (14.7 psi or 30 inHg) to near vacuum during the intake stroke, shown in Table A1. These pressures were measured using the manifold pressure sensor in the plenum.

Higher vacuum pressures within the chamber force air to move through the intake system at higher velocities. The air flow speed through the intake can reach up to Mach 1 (~300 m/s) at WOT. Using the 20 mm restriction at a characteristic diameter, this corresponds to Reynold's numbers between 60,000 and 400,000. In these flow regimes, relative roughness has a large effect on the frictional factor for the intake. Higher frictional factors reduce the volumetric efficiency of the engine, reduce air flow, and negatively affect peak performance.

The baseline design is made of turned aluminum. The surface roughness for turned parts can be as low as Ra 3.2 µm (Smoothy 2024), which corresponds to a relative roughness of 0.00016 for the 20 mm restriction. For untreated 3D-printed parts, the surface roughness is at best only a function of the layer height, and can be assumed to be half of the layer height. All the CF-ASA were printed at 0.16 mm layer height (lower heights compromise z-axis strength), which corresponds to a relative roughness of 0.004. However, after acetone smoothing, it is

difficult to assess the roughness for the processed 3D-printed parts without using an expensive surface roughness gauge. Notably, the processed surfaces are smooth to the touch, so we may assume that the relative roughness is at least an order of magnitude smaller, and comparable to that of turned aluminum.

3.1 Component Design

3.1.1 Air Filter

The ITG Maxogen JC62 air filter, used in the previous intake design, is also employed in the current system to facilitate accurate comparisons between designs, shown in Figure A1. As mentioned in Section 1.2.1, its performance is closely tied to the housing design, which has been iteratively developed and tested throughout the semester.

Multiple iterations of air filter housings were designed via CAD, and subsequently 3D printed and tested using a flow bench. All designs shared a few essential geometries to improve integration with other intake components. These include a top diameter of 70 mm, a bottom inner diameter of 36.022 mm, and a 10 mm outer wall that secures the base of the filter with a silicone coupling. These consistent dimensions allow the housing to house the filter and interface smoothly with the throttle body and venturi.

After several housing iterations, adjustments and flow testing, two housing designs demonstrated the best performance in terms of cubic feet per minute (CFM) airflow. Both were then tested with the ITG Maxogen JC62 filter mounted to evaluate combined performance. The final two designs and their cross-sectional views can be seen in Figures A3 and A4 respectively.

Housing #1 features a height of 70 mm and an almost conical wall shape with a slight curvature. This design tapers to a 7.2° angle at the bottom, matching the geometry of the throttle body.

Housing #2 incorporates a more complex geometry with a smaller height of 40 mm. The bottom 20 mm is conical with a 7.2° angle, while the top 20 mm transitions into an aggressive bellmouth shape. The angle between the top of the bellmouth and the horizontal is 8.0°.

Flow bench results, whether tested alone, with the filter, or attached to the entire intake system, showed nearly identical performance for both housings. For this reason, both designs will be retained for further testing when the full system is integrated into the car. Further testing on the dynamometer and on track will determine the final selection between these two designs.

3.1.2 Throttle

The main tradeoffs between a barrel and butterfly throttle are air flow and complexity. The barrel has better airflow since there is no restriction in the center of the throttle body. On the other hand, the butterfly valve has considerably fewer parts. To investigate these claims, both throttles were designed, simulated in CFD, 3D-printed, and flow benched. The flow bench results are shown in Figure A2. The printed throttles both have an inner diameter of 28 mm, equivalent to the diameter in the baseline throttle.

From the flow curves, the barrel throttle has slightly higher flow at low throttle angles but there is no significant difference between the two at high throttle angles. This indicates that the

plate restriction does not block significant flow at WOT. The difference in flow rates at lower throttle angles could be due to the clearances in the 3D-printed parts; there are more rotating parts in the barrel throttle and more area for clearances, allowing more air to flow around the barrels at low throttle angles. At high throttle angles, the flow rate is too high for the clearances to make a difference in flow.

Both throttle bodies were also simulated in CFD to visualize the flow through the valves. The intake components are designed for streamlined flow, since this promotes the fastest flow speeds. By analyzing the streamlines shown in Figure A3, the barrel throttle has more streamlined flow compared to the butterfly. There is also a smaller area of low pressure behind the two barrels than behind the butterfly plate.

Due to the desirable streamlined flow produced by the barrel throttle, we chose to pursue a barrel design for the final prototype. Although there is additional complexity and risk of jamming, a well-designed barrel should not add significant mass or risk to the function of the intake system.

The area of low pressure behind the barrels can be further reduced by applying a taper to the bore in the throttle body. The angle of the taper is matched to the converging angle on the venturi to reduce the disturbance of the throttle barrels at WOT. A cross-section of the tapered barrel throttle is shown in Figure 5.

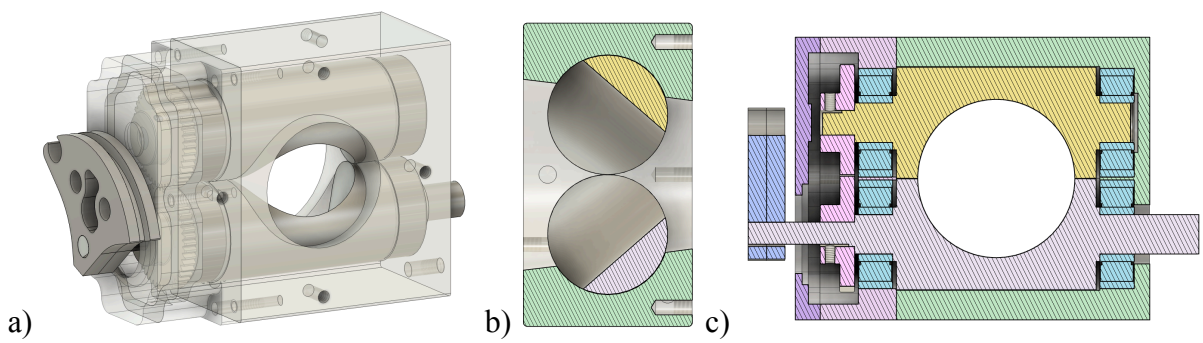

Figure 5. Tapered Barrel Throttle, shown at 70% throttle. a) Complete CAD of final prototype. b) Cross-section of the throttle, demonstrating the smaller wake behind each of the barrels. c) Axial cross-section of the throttle, with each component displayed in a different color: Barrel 1 (Yellow), Barrel 2 (Light Purple), Body (Green), Bearings (Teal), Acetal Gears (Bright Pink), Cover (Dark Pink), Lid (Dark Purple), Cable Cam (Blue).

The final taper barrel prototype is made from several custom components, machined from 6061 Aluminum, and several components bought from McMaster-Carr and Amazon. The bill of materials for the throttle is tabulated in the appendix. The throttle is composed of a stationary body, two rotating barrels, four 22 mm skateboard bearings, two acetal spur gears, a cover, and a cable cam.

The throttle should be lightweight, be able to rotate freely, and require little force to actuate (before the return springs are added). Therefore, the inertia of the rotating components should be minimized. The size of the barrels is bounded by the size of the taper bore; the bore is ~35 mm at the inlet, so the barrels must be at least half of that in diameter. Adding about a

quarter inch to this diameter ensures that the left and right sides of the barrel are rigidly connected. This results in a final barrel diameter of 22.5 mm. The barrels have a 0.06 mm (0.0024”) gap between each other, and 0.06 mm clearance from each surface to the body. This ensures the barrels do not slide against each other or the body during operation.

The two barrels are slightly different from each other. Both have half of the taper bore cut into the main section of the barrel. Both have an 8 mm boss on either side of the main section to accept the bearings. On top of the left boss, there is another 5 mm boss on top of the 8 mm boss to accept the gears. Using Figure 5 as a reference, there are no more features for the top barrel (Barrel 1) aside from those previously listed. The bottom barrel (Barrel 2) extends the 8 mm boss to the right, beyond the body and into the Throttle Position Sensor. The 5 mm boss is also extended to the right beyond the cover to connect to the cable cam.

Skateboard bearings were chosen since they are cheap, low profile, and are slightly under the diameter of the barrels. If the bearings were larger in diameter than the barrels, an additional cover would be needed to house the bearings, increasing the complexity and adding more tolerances that could increase the running torque of the system. To locate the bearings, a 0.001” interference gap is built into the body. The body is heated with a heat gun and the bearings are cooled in a freezer before being assembled. This retains the bearings and reduces the amount of radial and axial play.

Acetal spur gears with a pitch diameter equal to the barrels (22.5 mm) were chosen. The throttle only sees forces from the return springs and vibrational loads from the engine. Acetal was chosen for low density, high strength-to-weight ratio, and durability. The gears are post-processed by drilling and tapping an M3 hole in the shoulder of the gear to accept an M3 set screw. This set screw positively retains the gear to the barrel shaft.

The intake system is protected by a cover that retains a pair of bearings and a lid that provides a bit of preload onto the barrels. The acetal has a low coefficient of friction with aluminum, so the barrels can still rotate under the preload.

The cable cam is designed to reduce the rate of throttle change at low throttle angles, and gradually increase the rate of throttle change at higher throttle angles. This is to increase the driver’s control over the engine at low speeds. The total angular travel of the throttle is 110 degrees from closed to WOT. This is greater than the ~85 degrees of travel for the baseline butterfly throttle. As a result, the radii of the barrel cable cam must be smaller than the butterfly cable cam to preserve the same linear range of motion in the cable itself.

At the time of writing this report, the barrel throttle has not been fully machined. The fully machined throttle will be ready by the start of the spring semester. The progress on the throttle is shown in Figure A7. However, this did not delay full stack testing because a placeholder barrel, printed in PLA, was used instead. As a result, the flow bench measurements may not be accurate for the machined throttle, but will at least give us an idea if we are moving in the right direction.

3.1.3 Venturi

The new venturi was a drastic improvement from the baseline venturi. 3D printed with Carbon Fiber - ASA filament, this design addressed all the design constraints and found, as it

seems, almost fully optimized results during testing. As seen in Figure 6, the cross-section and detailed sketch have the lengths, angles, and radii of the converging and diverging sections. Another design detail we decided on was a 6.00mm fillet to make the flow through the restriction as smooth as possible. The parameter measurements of the venturi are:

Parameter	Converging (Inlet)	Diverging (Outlet)
Angle	14.4 (7.2) degrees	10 degrees
Length	32mm	86.011mm
Diameter/Radii	28mm/14mm	35mm/17.5mm

a) 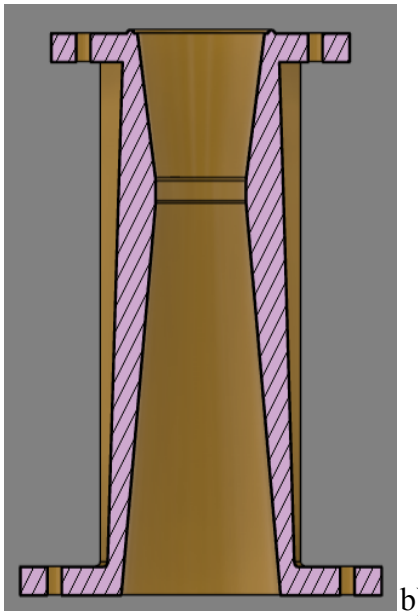 b) 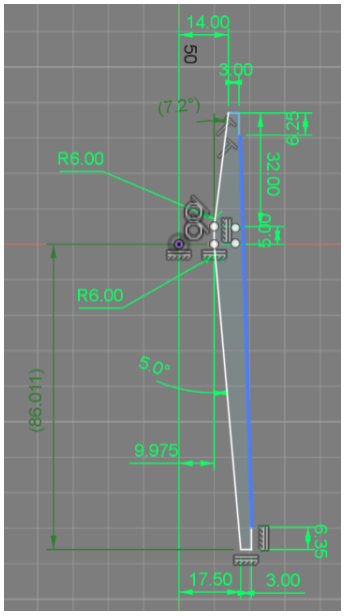

Figure 6: New Venturi Model a) section view to show detailing of design b) sketch showing specific parameter measurements

The baseline model had a similar shape with direct converging and diverging sections but had a longer converging section than the diverging section. This seemed to be the most impactful limiting factor of the baseline model, so the first change was reversing this design and making the diverging section longer than the converging section. This was reflected in many research papers on venturis, as a shorter diverging section does not benefit from the venturi effect as much as the latter. During flow bench testing, 7 CFM in mass flow was gained in the first reversed version, which was an inversion of the baseline model with larger angles for convergence and divergence.

When improving upon this design, the constraints from the throttle body outlet (28mm diameter) and plenum inlet (35mm diameter) had to be considered. This limitation allowed the focus to be set on the length and angle for both sections, which were dependent on one another and reflected in the new venturi. The second version of the reverse model used a 14-degree angle (7 on each side) and was 32mm in length for the converging section, while the diverging section

used a 10-degree angle (5 on each side) and was 60mm in length. This yielded an improved airflow of 72 CFM at a pressure of 10inHg. The issue with the second version was it was not optimized for the constraints of the plenum mentioned above. This led to the new model with the same angle, but a longer diverging section of 86.011mm. The testing results yielded a maximum of 73 CFM for airflow. Although this was an improvement from version two, the resulting conclusion was that the length of the diverging section does not matter much, as long as it exceeds greatly exceeds the amount of the converging section.

In light of further increasing the mass flow rate, the 3D printed designs had air leakage through the layer lines. To maximize flow, we opted to acetone smooth each part. Not only did it address air leakage, but it also smoothed the surface yielding a 10% increase from the unsmoothed model, resulting in a 77 CFM.

Most of the testing for the venturi was conducted on the flow bench, but due to the inability to test at Mach 1 speeds (sonic flow), a computational method, Comsol CFD, was used to understand the behavior at those flow speeds. Figure 8 displays our Flow Bench test results for each printed design. The flow bench is always operated in the intake settings and tested at approximately 2.5, 5, 7.5, and 10 inHg for each model. The Flow Bench Results displays only the reversed and baseline designs to show the progression of the relevant results. There were two other design configurations mentioned previously, but the models yielded results that were below the baseline

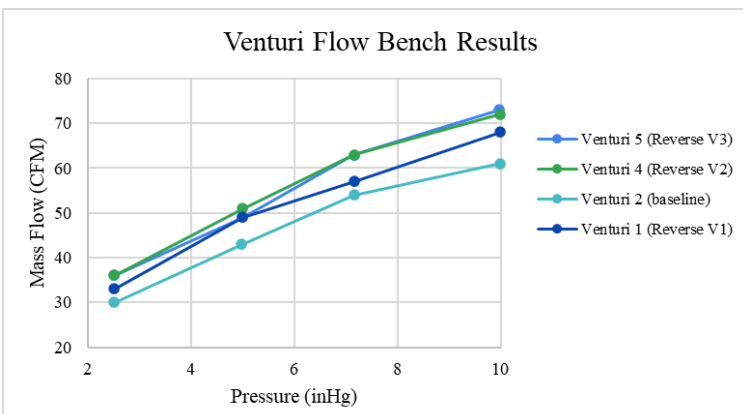

Figure 8: Venturi Flow Bench Results of the Baseline Model and the three reverse venturi showing improvement in the design.

The testing process of the venturi was spread out as models were improved and updated. From baseline to Venturi 5 (Reverse V3), the new and finalized design, there was an average of 17.6% increase in Mass Flow, as seen in the table below**.** The baseline testing resulted in 61 CFM at 10inHg. With the Reverse Venturi V1, the mass flow jumped to 68 CFM. In comparison to the other configurations tested, in the first round of designs, this was the only design that yielded improvement. In versions 2 and 3 there was an increase of 4-5 CFM, which is where it was found that the length of the converging section was not impacting the airflow to the extent that was originally believed.

Baseline to New	**10 inHg**	**7.5 inHg**	**5 inHg**	**2.5 inHg**	**Average**
Percent Increase	19.7%	16.7%	14.0%	20.0%	17.6%

To further increase mass flow, acetone smoothing sealed leakage through the layer lines and improved surface roughness. This involves sanding the part for any large defects that the acetone smooth would not change, submerging the part in a sealed container of acetone for 15-30 seconds and setting it to dry for 90 seconds. During the testing process, an unsmoothed venturi was used as a baseline, which had a flow rate of 70 CFM. After this, two venturis were submerged for 15 and 30 seconds. The flow bench yielded the same results of 77 CFM, which proved that as long as there was enough time for the reaction to occur, the submergence time did not affect the results. Moreover, the acetone smoothing made a 10% increase from the unsmoothed model and a 5% increase from the PLA-tested model, so it was decided that this would be the best way to address the layer leakage and surface roughness.

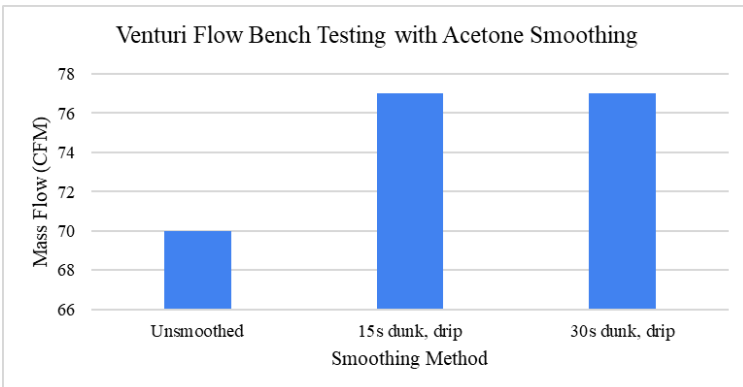

Figure 9: Acetone smoothing flow bench test results

Finally, CFD was used to verify the results at higher flow speeds. The parameters were fully developed flow at the inlet at an average velocity of 100m/s and -85,000 psi at the outlet which was a reasonable estimate from plenum testing. This results in speeds closer to the sonic threshold, but an outward mass flow rate of 0.0729kg/s exceeding the choke flow maximum. This may have occurred because of the lack of inlet and outlet parameter knowledge, but it does prove that the there are better results with our design, but there is a lack of specific parameter knowledge. The CFD modeling is something to be improved in the coming semester.

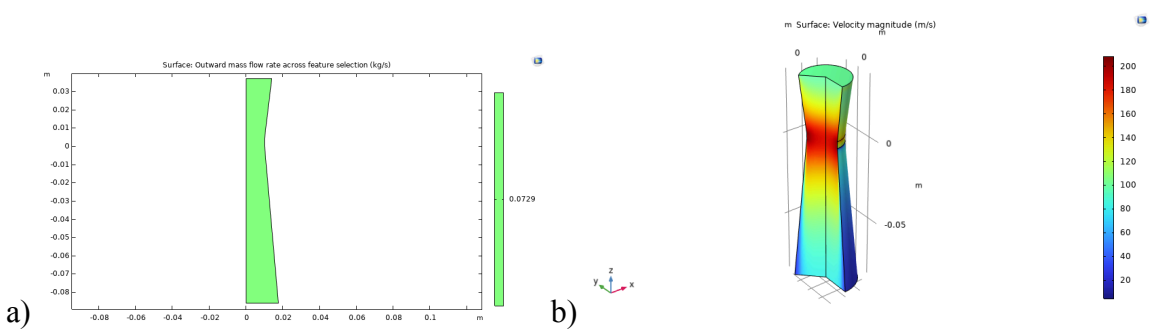

Figure 10: a) Outward mass flow rate of 0.0729kg/s for new venturi model b) Velocity profile through the venturi with speeds through the restrictor around 200 at maximum.

Fortunately, the design itself poses no major risks, especially due to the plenum being the most susceptible to implosion from the vacuum pressure. However, the entire intake system may be susceptible to damage or melting due to its proximity to the exhaust. Although the CF-ASA filament has a higher heat tolerance than the originally posed, CF-ABS, the material could be a potential risk. To address this concern, the option of creating housing or a simple barrier between the intake and exhaust will be considered and, most likely, implemented. Another concern is acetone smoothing. Acetone is highly flammable and potent. With this, we take the needed precautions of conducting procedures in a safe place and wearing masks and eye goggles for protection.

3.1.4 Plenum

Since the hoop stress is proportional to vessel diameter, the plenum experiences the greatest loads of any component in the intake. Therefore, a vacuum pressure test was performed to determine the wall thickness required to withstand 25 inHg pressures.

A pressure vessel with an internal volume of 1545 cc (same as the volume of the baseline plenum) was initially printed in CF-ABS at the Digital Fabrication Lab, shown in Figure A10. This plenum was optimized for 3D-printed–no overhang angle is greater than 50 degrees–causing the plenum to appear prolate. The printed plenum has an internal diameter of 150 mm, corresponding to a hoop stress of:

$$\sigma = \frac{PD}{2t} = \frac{(30\ inHg)\ (0.15\ m)}{2\ (0.005\ m)} = 762\ kPa \qquad \sigma = \frac{PD}{2t} = \frac{(30\ inHg)\ (0.15\ m)}{2\ (0.001\ m)} = 152\ kPa$$

Even with a 1 mm wall, this is several orders of magnitude below the yield strength CF-ASA i.e. the safety factor is extremely high. However, if the walls become too thin, the pressure vessel may buckle under the compression loads and vibrational loads the vehicle exerts while in motion. Thin walls are also more difficult to print consistently, and make it easier for air to seep between the layer lines. Therefore, a wall thickness of 3 mm was chosen for all the components in the intake system, but walls less than 3 mm can be tolerated in some regions if demanded by other constraints.

The plenum is sealed on the top interface with an aluminum plate and epoxy. The bottom interface is sealed with a face plate and O-ring or gasket. The face plate has 4 bolts, an O-ring groove, and is machined to a smooth finish. The plenum is fitted with a hose barb and vacuum pressure gauge. To ensure that air does not leak into the plenum during the vacuum test, a leak test was performed, shown in Figure A11.

For the leak test, the NPT threads for the barb and gauge are wrapped with teflon tape to ensure a tight seal. The bottom interface of the plenum was fitted with an O-ring or gasket. Compressed air is then pumped into the plenum and dunked in a bucket of water. At +6.1 inHg, air started leaking from layer lines and O-ring seal. The plenum was depressurized, and gasket placed on top of the O-ring. The plenum was repressurized. At +10 inHg, air started leaking from the edges of the gasket. No air leaked from the NPT threads during both trials. This test demonstrated that acetone smoothing would be required to further seal the layer lines together.

This also demonstrated that four bolts were not enough to seal the large outlet diameter, so more bolts would be needed in future plenum designs.

Since the positive pressure is pushing the gasket out and expanding the seams in the layer lines, we hypothesized that negative pressure would help seal the plenum by increasing the preload on the gasket and shrinking the seams in the layer lines. Thus, this proved to us that we could proceed to vacuum testing, and verify that the plenum could hold a minimum of 10 inHg of vacuum.

For the vacuum test, the pressure vessel was lightly clamped (to clock the vacuum gauge for better visibility) and placed behind blast shielding. A roughing pump was connected to the plenum and turned on. The pressure in the plenum dropped to -30 inHg and was left for several minutes. The pump was then turned off, and the plenum pressure remained the same. The vacuum line was then disconnected to simulate a pressure wave from the engine. The plenum did not sustain any visible damage during testing.

After vacuum testing, the plenum was flow benched, and tabulated in Table A2. Due to the bulbous shape, air slows down after entering the plenum, negatively affecting the mass flow rate throughout the plenum. The plenum was initially designed for a 23.4 mm inlet (the same size as the AT Power venturi outlet). However, this led to a flow rate of 37 CFM, lower than the venturi itself. By expanding the inlet diameter (we cut off the top of the plenum), a 32.8 mm inlet was found to flow the same as the venturi. Greater inlet diameters may have increased the flow rate of the plenum, but would require the venturi length to increase considerably to meet the interface diameter.

A second plenum with 753cc (which is 1.5 times the engine displacement), was printed out of CF-ASA, with an internal diameter of ~80 mm, a wall thickness of 3 mm, inlet of 32.8 mm, and a 6 bolt pattern for the bottom interface. This second plenum was flow benched, and performed better than the first plenum with the modified inlet. This is due to the smaller bulb/diameter, leading to more streamlined flow. No further tuning was performed since plenum volume and shape tuning requires full-stack testing on the car to determine how much lag the system has.

3.1.5 <u>Runner</u>

As briefly outlined in a preliminary introduction to the purpose of the runner, several parameters were optimized over the past three months of iteration and testing. Different runner designs yielded a variety of flow benching results. The first runner tested was a 13 cm long, aggressively rifled runner, which had performance that bestedits non-rifled counterpart at specified ranges. To optimize this, the runner was made to feature a balance of the rifling feature, where the profile was made less aggressive and prominent, and the number of spirals was decreased.

Similarly, when testing the 13 cm and 6 cm long runners, their results also had specific ranges at which either would top the other in flow (CFM). Another balance was made with the final design, where the benefits of the long and short iterations were molded into one design at 7 cm long. The most critical aspect of the runner development process was the use of flow bench testing to quantify performance, as alluded to with CFM measurements. Each design iteration

was subjected to a series of controlled tests measuring airflow in cubic feet per minute at multiple pressure differentials – namely 2.51, 5, 7.16, and 10 inches of H2O. The data collected from these tests was used to create flow performance curves, highlighting which designs excelled at specific operating conditions. This data-driven approach allowed for a systematic refinement of the runner geometry, avoiding the trial-and-error guesswork that often plagues early-stage development.

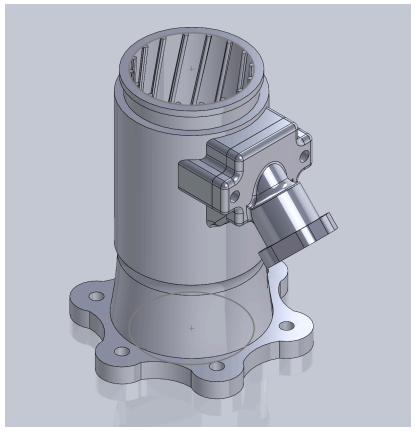

Figure 11: Final runner CAD Model

The theoretical flow that this runner will achieve stands at 156 CFM, a 16 CFM increase over the first iteration of its kind and what is expected to be an increase over the existing runner that is currently used for the racecar. Paired with the rest of the intake assembly, the optimized runner is expected to significantly contribute to an increase in performance of the car and will likely ease the process of repair and service.

Holistically, it is possible that the runner will have either increased or decreased performance when applied to the racecar and in a race-setting. Factors such as vibration, air temperature, and stress and strain from the car's cornering may slightly alter the shape, rigidity, and behavior of the runner and its interior features. Until a test with the full assembly attached to the race car and on a dynamometer, theoretical results will only lend insight into how the runner might perform and the conditions at which 156 CFM is possible.

3.1.6 Gaskets, and Hardware

To ensure the full stack had a smooth and continuous interior surface, all the inlets and outlets between each component must be matched. As the inlet and outlets were changed on one component, the changes were mirrored in adjacent components to ensure the bores would match. One of the main issues faced by the Motorsports team during competition was the entire intake system rotating about its axis, creating tension on the throttle cable. To address this, bolts are used to fasten each component together, rather than press fits.

Due to the vacuum pressure experienced by the intake, the gasket seals between each component fall under ANSI Class 150 for pipe flanges (American Society of Mechanical Engineers 2021). Gaskets used for these flanges must be preloaded to 600 psi. Grade 5 No. 6 (#6-32 SAE) fasteners were chosen to apply this pressure due to their design clamp load (580

lbs). The equation for this decision is shown below, and gasket pressures for each interface are shown in Table A3.

$$\sigma = \frac{(\#\ bolts)\ (Preload)}{(Flange\ Area)}$$

Specifically, Grade 5 #6-32 Zinc-Flake coated Socket Head fasteners were chosen. The zinc coating prevents corrosion from rain. The socket heads were chosen for use with Allen keys. Due to the overhanging geometries of the components, it is difficult to use spanner wrenches or larger tools to tighten the bolts. Ball-end Allen keys are ideal for these applications; socket heads fasteners are used in several other areas on the car for this reason. Since the socket heads have a very small shoulder to distribute load, oversized steel washers are used to evenly distribute the preload across the component flanges. Grade 5 flex top nuts are used to positively retain the fasteners once tightened.

The gaskets themselves are laser cut from a sheet of 0.125” Neoprene rubber, shown in Figure A12. The rubber is water resistant and chemical resistant. Viton rubber sheet was laser cut for the O-ring in the fuel injector boss due to the higher fuel resistance of Viton rubber.

3.2 Analysis of Complete Design

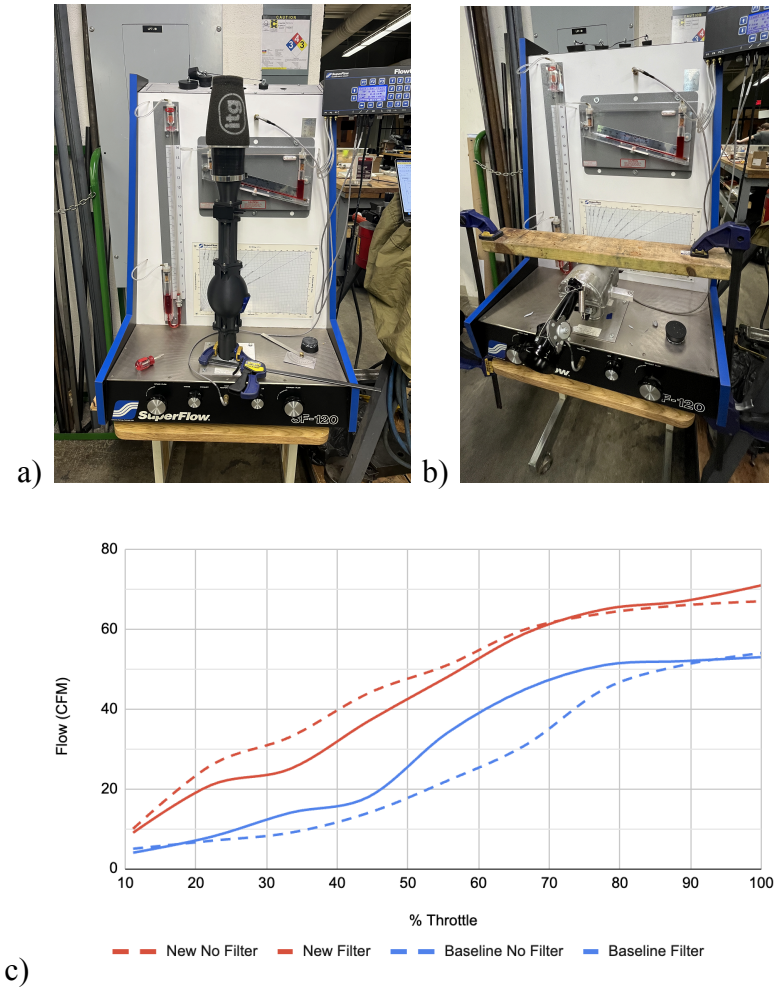

Figure 12. Full-Stack Flow Bench Testing. a) New system. b) Baseline system. c) Flow Curves for both systems, with and without the air filter attached.

Once final prototypes for each component were completed, a CF-ASA version was printed (and placeholder PLA version for the throttle). The components were assembled with gaskets, and prepared for flow benching by blocking off the plenum orifices and fuel injector hole. The flow bench was run at 10 inWg test pressure, and throttle angle varied from 10% to 100%. The baseline intake system was tested with the same parameters. The test setup and results are shown in Figure 12.

In general, the new system performed significantly better than the baseline system. At WOT, the existing system flowed 53 CFM and the new system flowed 71 CFM. This represents a 34% improvement in flow rate from the baseline system. At lower throttle angles, the new system also performs significantly better, representing a 25-30% improvement. Furthermore, the flow curves closely match the area curves shown in **Section 1.2.2**. There are some inconsistencies between the flow curves and area curves. For example, at 25-35% throttle, there is a flat spot in the flow curve, indicating that the resonances in the system may be choking flow at those throttle angles. These flat spots will be addressed in future designs.

Most importantly, the peak CFM of the system is within 2% of the peak venturi flow rate. This indicates that the rest of the system does not negatively affect flow any more than the restrictor does. The 2 CFM difference could be due to the presence of additional burrs and print defects that need to be sanded down before acetone smoothing. After acetone smoothing all of the CF-ASA parts, we expect the new system flow rate to peak around 77 CFM, representing a 45% improvement from the baseline system.

3.3 DBT 2 Outcomes

At the time of writing this report, there is no additional testing with the full-stack. However, the progress made this semester demonstrated great strides in meeting the three goals outlined in the Introduction.

The final prototype intake system represents a 34% improvement in flow rate compared to the baseline system. Once attached to the car, the volumetric efficiency of the engine should increase dramatically, increasing the peak power and peak torque of the vehicle at all RPMs.

The robustness of the system was demonstrated in leak testing and vacuum testing. The 3D-printing fabrication method was proven to be airtight, and handle the vacuum pressures generated by the engine. Furthermore, using 3D-printing for prototyping reduces the system complexity since fewer machining steps are required to fabricate each component.

4. Next Steps and Lessons Learned

In the coming semester, the goals for the project will shift towards integrating the intake system onto the car, and tuning the components to reduce input lag.

As part of integration, the intake system will have to take on a curved shape to wrap around the car. Currently, the new intake system will stick out the back of the car, extending beyond the 'Tire Envelope' of the vehicle, which is prohibited by the rules. The length of the system also makes it difficult to support; in high-G-force cornering, the polar moments generated may cause the intake system to disconnect from the engine, exposing the engine to atmospheric pressure, creating a runaway engine scenario that will endanger the driver and vehicle.

To address this, the intake system must be rigidly connected to the vehicle chassis and ensure that scenario does not occur. This may require curving the runner and plenum to wrap around the chassis, making it easier to design supports for the intake system. Furthermore, wrapping the intake system will locate the air filter in 'clean' air i.e. air that does not have significant turbulence. Clean air is typically found in regions on top of the driver's helmet or to either side of the vehicle roll hoop. This clean air can also provide a ramming effect, increasing the pressure in the intake system, and further increasing volumetric efficiency.

The intake system is only one system in the powertrain. The dynamics of the engine and exhaust system also play a pivotal role in the overall performance of the vehicle. Tuning the engine for the higher volumetric efficiencies of the car will be necessary to maximize performance for our new system. Furthermore, modifying the exhaust system to prevent back pressure from entering the intake is also important for maximizing the amount of fresh air-fuel mixture in the combustion chamber. As the full-stack intake is tested on the car, modifications will be made to both of these systems for maximum performance.

The design and testing of the air filter housing taught us the importance of iterative development and precise design for optimizing airflow and compatibility with the intake system. Flow bench testing demonstrated that even subtle changes in housing shape could significantly impact performance, leading to the retention of two top designs for further testing. A surprising takeaway observed after testing is the improvement in overall airflow performance with the air filter mounted on, something that the team initially thought would be the opposite. These lessons will guide future iterations as the intake system is integrated onto the car and tested as a complete assembly.

The complexity involved with a taper barrel throttle body was demonstrated during the design phase. With so many design decisions to make, two designs were made and printed before a third model was finalized and chosen for machining. However, by putting more hours into the design process, less time will be needed to troubleshoot and redesign in future design cycles. Machining the throttle has been a great experience for learning computer aided manufacturing (CAM), and how to create efficient tool paths. In the coming semester, the taper barrel throttle will be machined, and the full-stack can be mounted on the car for dynamometer testing.

The venturi was a component of little change, but large impact. When analyzing and designing this component it was interesting to see how changing the shape on the converging and diverging section either significantly decreased the performance or brought it down to the baseline performance. However, this proved ineffective and limited the baseline model to the entire system. To our surprise, the best design was simply reversing the baseline model and slightly adjusting the angles, length, and diameter of the converging and diverging sections. This discovery streamlined the process of designing for drastic improvement to the system because there were not too many parameters that needed to be addressed. Sticking to simplicity seemed to be the best option to avoid losing track of improvements versus limiting factors. Moving forward, the only way to further optimize the venturi is to test on the car, understand the behavior, and further tune the component. This being said, the goal is to surpass 80 CFM through the venturi, to minimize the loss through the other components.

5. Conclusions

This DBT cycle represents a major step in the right direction for designing the intake system. The final prototype intake system represents a 34% improvement in flow rate compared to the baseline system, which correlates to a higher volumetric efficiency once mounted on the car. The system is robust and capable of handling the vibrational and vacuum loads imposed onto it, without leaking. The 3D-printing fabrication method was demonstrated to excel for rapid iteration.

In the coming semester, we aim to prove the claims of higher engine performance, and further tune the intake system to reduce lag and improve peak power. The intake system will also be better integrated with the vehicle chassis to both be rules compliant and take advantage of the ramming effect.

6. Engineering Design Considerations

ABET Outcome 2	Design Considerations:
Public health	Machining and 3D-printing produce waste material that cannot be recycled. Aluminum chips are seldom recycled and CF-ASA support waste cannot be recycled without compromising the strength of the recycled filament. This waste material ends up being burned in landfills, reducing air quality.
Safety	Machining is an inherently dangerous fabrication method; proper training is required for operation. 3D-printing ASA releases styrene gas, a carcinogen, that must be filtered out by HEPA filters. Acetone is highly flammable and is a skin irritant; proper handling is required.
Welfare	Improving engine performance increases the welfare for the race car drivers.
Global factors,	Aluminum stock and CF-ASA filament is readily available on the market, allowing this design to be produced at scale.
Cultural factors	Intake systems have been studied for over a century, so the aerodynamics are well understood. However, new fabrication methods, like multi-axis machining and 3D-printing, open doors to new designs that were never possible in the past.
Social factors	Intakes system must prioritize safety, accessibility, sustainability, affordability, and cultural relevance, while minimizing environmental impact and addressing the needs of the drivers
Environmental factors	The system must minimize environmental impact by reducing styrene emissions, optimizing energy efficiency to lower operating costs in compliance with regulations
Economic factors	Low cost for full design, build, and testing this is reflected in the bill of materials for complete system

ABET Outcome 4	How your design solutions impacts:
global contexts	Any combustion-engine machine or vehicle can benefit from optimized airflow for the combustion process. This design takes advantage of new fabrication techniques that are not traditionally see in automotive engineering.
economic contexts	Fuel efficiency can lend to DOE and EPA tax credits for companies and people. Increase engine efficiency reduces consumer prices.
environmental contexts	More efficient combustion via optimized airflow as well as minimal-waste fabrication have the potential to revolutionize manufacturing and the ICE engine, even beyond shifts in fuel sources from fossil to synthetic combustible fuels.

societal contexts	The automotive industry is on the forefront of cutting edge technology. New records in engine performance impact cultural appreciation of new technology and their applications to broader society.

7. Appendix

References

American Society of Mechanical Engineers. 2021. *Pipe Flanges and Flanged Fittings: NPS 1/2 Through NPS 24 Metric/inch Standard*. N.p.: American Society of Mechanical Engineers.

Bambu Labs. 2024. "ASA-CF." Bambu Labs Store. https://us.store.bambulab.com/products/asa-cf.

FS Wiki. 2023. "Throttle." FS Wiki. https://fswiki.us/Throttle.

Hillier, Victor Albert W., and Frank W. Pittuck. 1972. *Fundamentals of Motor Vehicle Technology*. N.p.: Hutchinson.

SAE International. 2024. *Formula SAE Rules 2025*. 1.0. https://www.fsaeonline.com/cdsweb/gen/DocumentResources.aspx.

Singhal, Anshul, and Mallika Parveen. 2013. "Air Flow Optimization via a Venturi Type Air Restrictor." IAENG. https://www.iaeng.org/publication/WCE2013/WCE2013_pp1847-1851.pdf.

Smoothy, Luke. 2024. "Surface Roughness Explained | Ra Roughness Chart." Get It Made. https://get-it-made.co.uk/resources/surface-roughness-explained.

Speed Talk. 2008. "Intake Plenum Volume." Don Terrill's Speed Talk. https://www.speed-talk.com/forum/viewtopic.php?t=13710.

Bill of Materials and Budget

Item	Notes/Use	#	Unit Cost	Total Cost	Supplier	Link
1/4" Barb to 1/4" NPT Male	Pressure sensors on plenum	1	$7.99	$7.99	Amazon	https://a.co/d/7yP5m35
1/4" Barb to 1/8" NPT Male	Adapter for fuel tank sensor	1	$6.99	$6.99	Amazon	https://a.co/d/i0LUR7v
3/8" NPT Plug	Sealing plenum during vacuum testing	1	$8.99	$8.99	Amazon	https://a.co/d/8NaVsxQ
Vacuum Gauge, 1/4" NPT Male	Measure pressure in plenum	1	$9.99	$9.99	Amazon	https://a.co/d/drn8dVJ

Neoprene Sheet 2'x2'	Making custom gaskets	1	$20.93	$20.93	McMaster	https://www.mcmaster.com/8525T34/
#6 oversized washer	Intake system sealing	1	$5.70	$5.70	McMaster	https://www.mcmaster.com/91525A104/
#6 flex top lock nuts	Intake system sealing	1	$15.49	$15.49	McMaster	https://www.mcmaster.com/94820A215/
#6 x 1" bolts	Intake system sealing	1	$16.15	$16.15	McMaster	https://www.mcmaster.com/91274A028/
#6 Bottoming Tap	Tapping #6 blind holes	1	$7.58	$7.58	McMaster	https://www.mcmaster.com/2636A63/
#4 Bottoming Tap	Tapping #4 blind holes	1	$9.87	$9.87	McMaster	https://www.mcmaster.com/2636A61/
M4 Bottoming Tap	For tapping TPS blind holes	1	$10.87	$10.87	McMaster	https://www.mcmaster.com/26475A78/
#6 Heat Set Insert	Heat set inserts for fuel injector	1	$7.25	$7.25	McMaster	https://www.mcmaster.com/97163A143/
Polymaker PLA	For iterating designs/prototyping	1	$30.00	$30.00	Polymaker	https://us.polymaker.com/collections/pla
Bambu CF-ASA	For final prototype printing	1	$36.99	$36.99	Bambu Labs	https://us.store.bambulab.com/products/asa-cf
6061 Aluminum Stock	For machining throttle	1	$45.00	$45.00	Motorsport Shop	NA
CAM and CNC Hours	For machining throttle	24	$30.00	$720.0	NA	NA
Slicing and Printing Hours	For printing components in CF-ASA	80	$11.00	$880.0	NA	NA
Assembly	For full stack integration, fastening bolts	2	$30.00	$60.00	NA	NA
Total Material and Labor Cost				**$1,899.79**		

Project Timeline

Detailed meeting notes are kept in our shared drive. Summary of progress, broken down month by month:

1. September: group formation, project introduction, brainstorming, initial task distribution, research, meeting with Phil, initial CAD and CFD work.
2. October: 3D printing, DBT 1, flow bench tests, design optimization, PDR.
3. November + December:

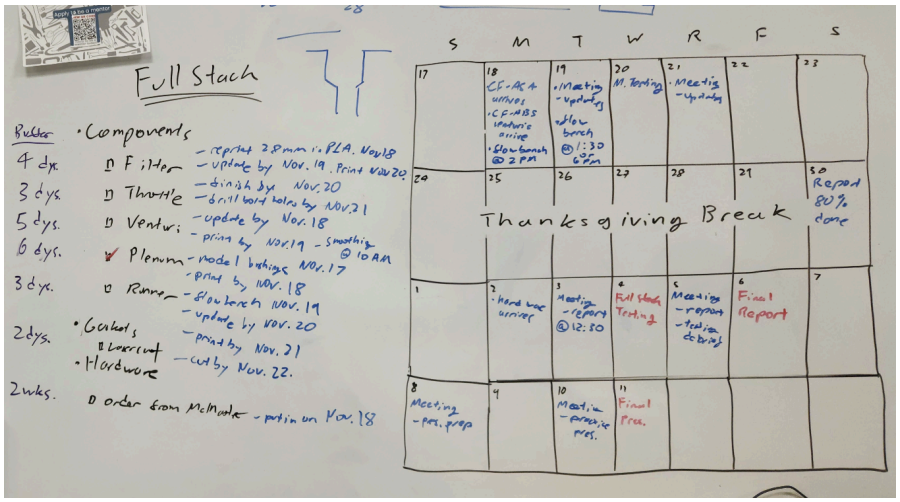

Tables

Table A1. Engine Vacuum

Engine Function	Vacuum Range
Cranking	3-5 inHg
Idle	14-20 inHg
Cruising	10-15 inHg
Deceleration	21-25 inHg

Table A2. Plenum Inlet Tuning on Flow Bench

Test Pressure	Plenum 1 (23.4 mm) CFM	Plenum 1 (32.8 mm) CFM	Plenum 2 CFM
10 inWg	37	74	94
7.5 inWg	34.5	66	82
5 inWg	28	52	72
2.5 inWg	21	37	46

Table A3. Gasket Preload for Grade 5 No. 6 Fasteners

Interface Area	Flange Area (sq. in)	# Bolts	Gasket Stress (psi)
Filter-Throttle	2.21	4	1048
Throttle-Venturi	1.46	4	1592
Venturi-Plenum	3.95	4	587
Plenum-Runner	4.33	6	785

Figures

Figure A1. ITG Maxogen JC62 air filter

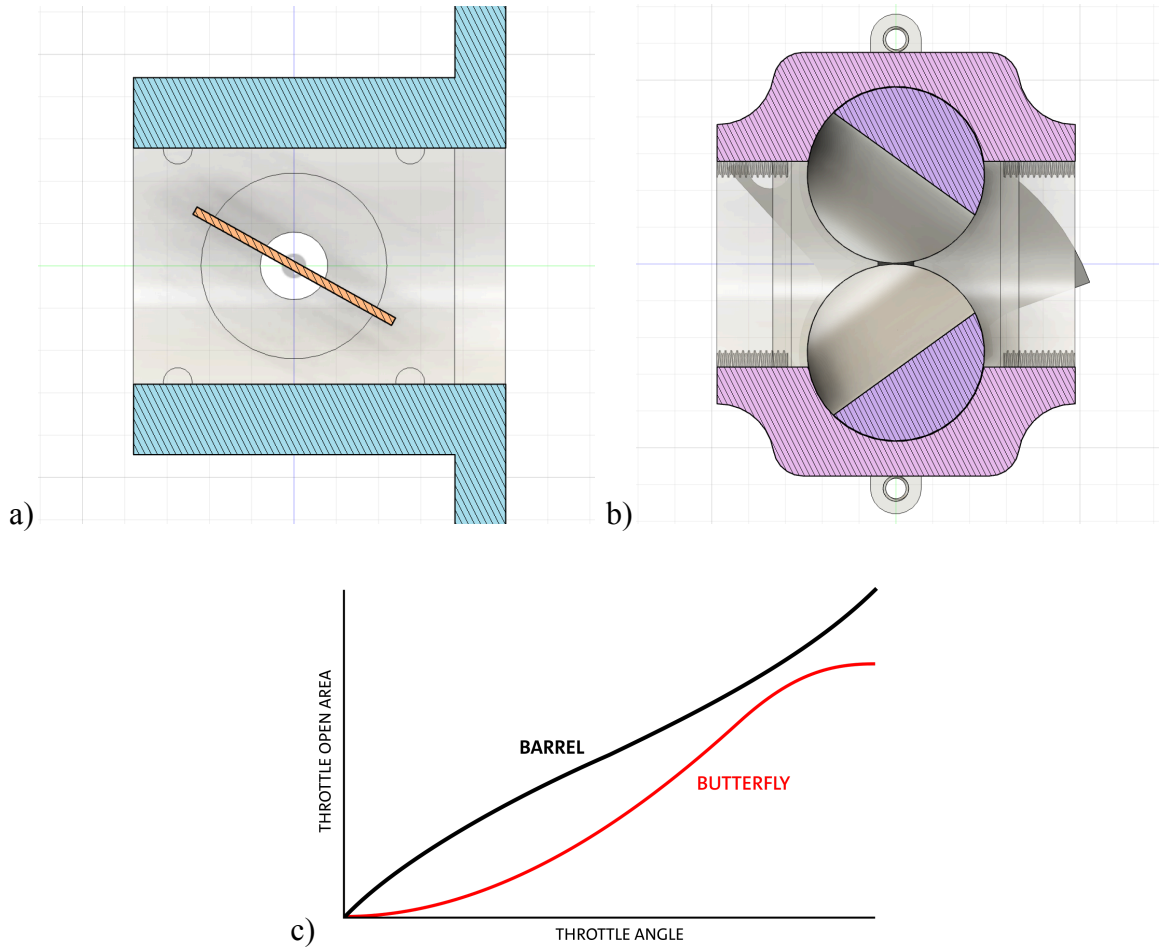

Figure A2. Cross sections of throttles at ~70% throttle. Inlet on the left of each image, outlet on the right. a) Butterfly throttle. b) Barrel Throttle. c) Throttle cross-sectional area as a function of throttle angle (FS Wiki 2023).

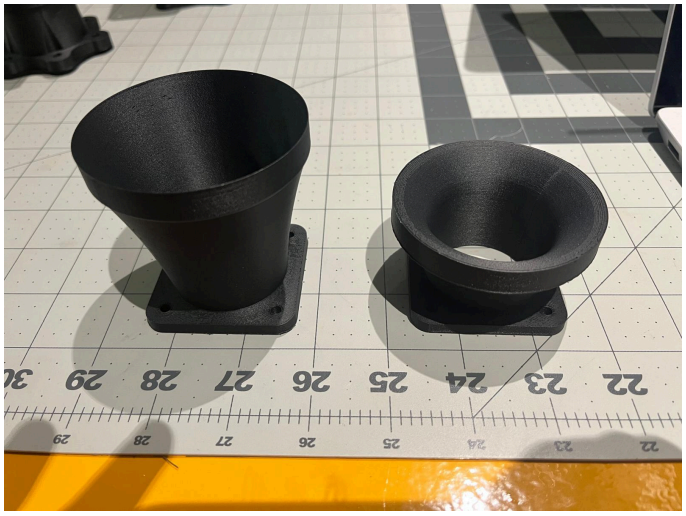

Figure A3. Side-by-side of air filter housings #1 (left) and #2 (right).

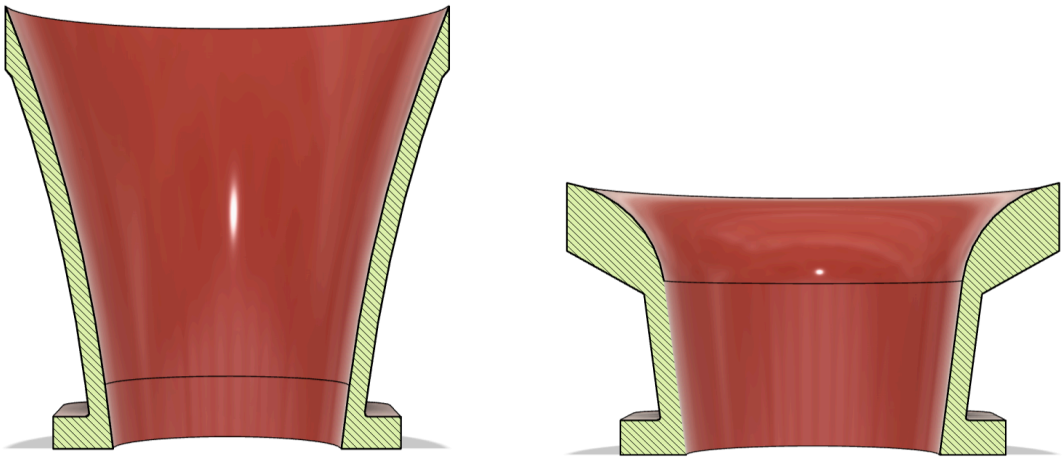

Figure A4. Cross sections of air filter housings #1 (left) and #2 (right).

Figure A5. Superflow SF-120 flow bench, equipped with the digital FlowCom interface.

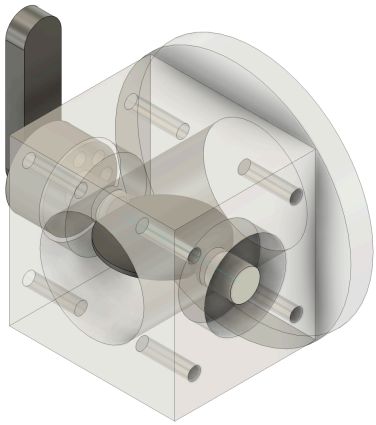

a)

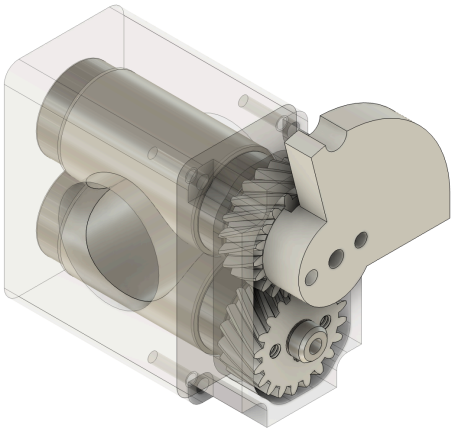

b)

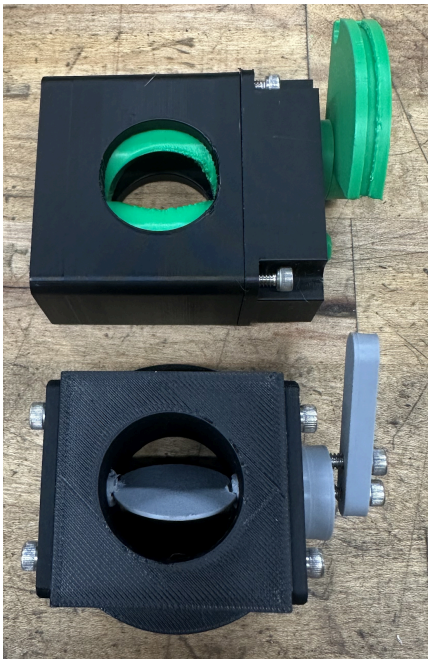

c)

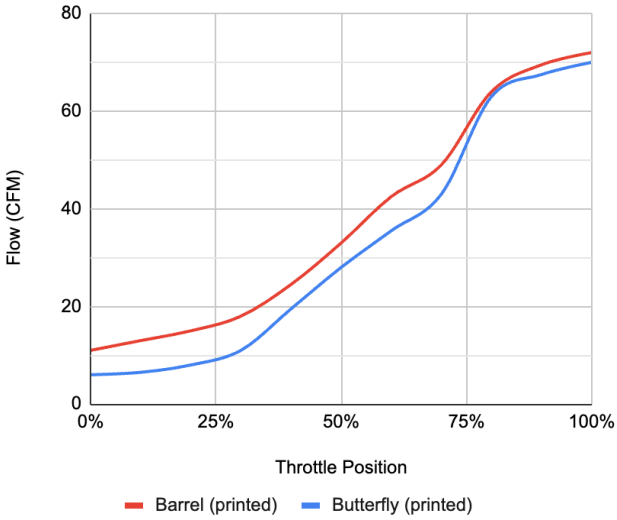

d)

Figure A6. Throttle Bodies and their Flow Curves. a) Butterfly throttle CAD. b) Barrel throttle CAD. c) 3D-printed throttles. d) Flow Curves for each throttle.

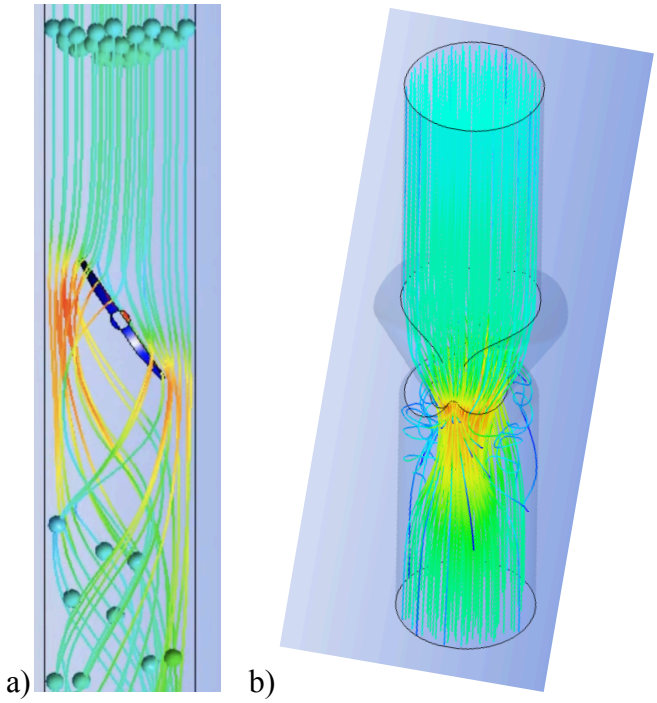

Figure A7. Throttle Bodies and their Streamlines at 30% throttle. Inlet is on the top, and outlet on the bottom. a) Butterfly throttle CFD. b) Barrel throttle CFD

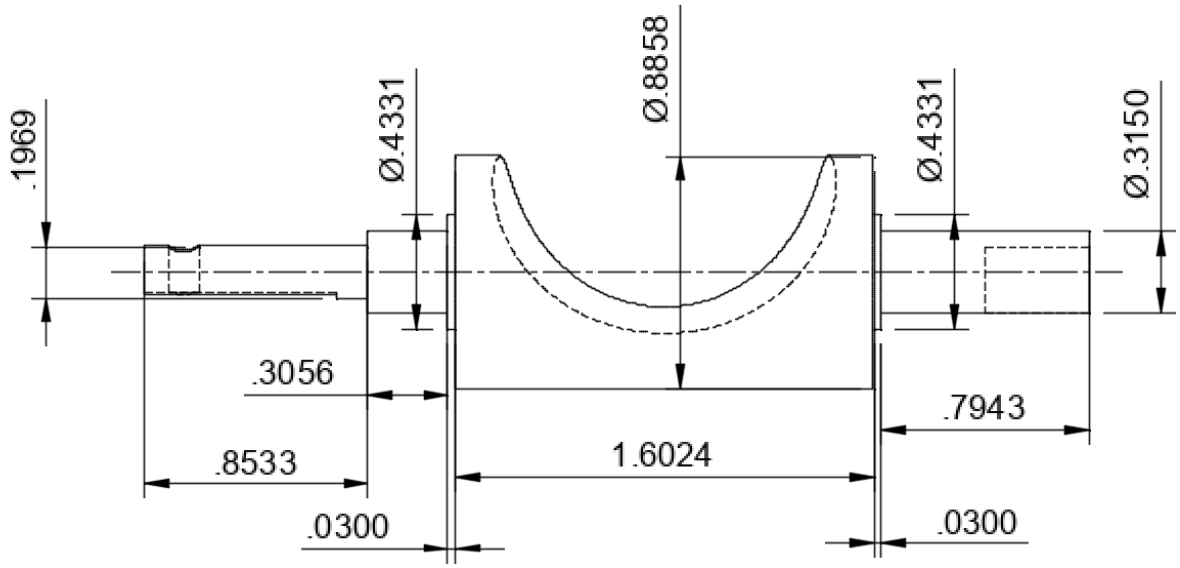

Figure A8. Dimensioned Drawing for Barrel 2. Unit is inches.

Figure A9. Taper barrel throttle machining progress. Seven more machining operations are needed to complete the design. [From Top Left to Bottom Right] Barrels, Bearing, Body, Cover, Lid, and Cable Cam.

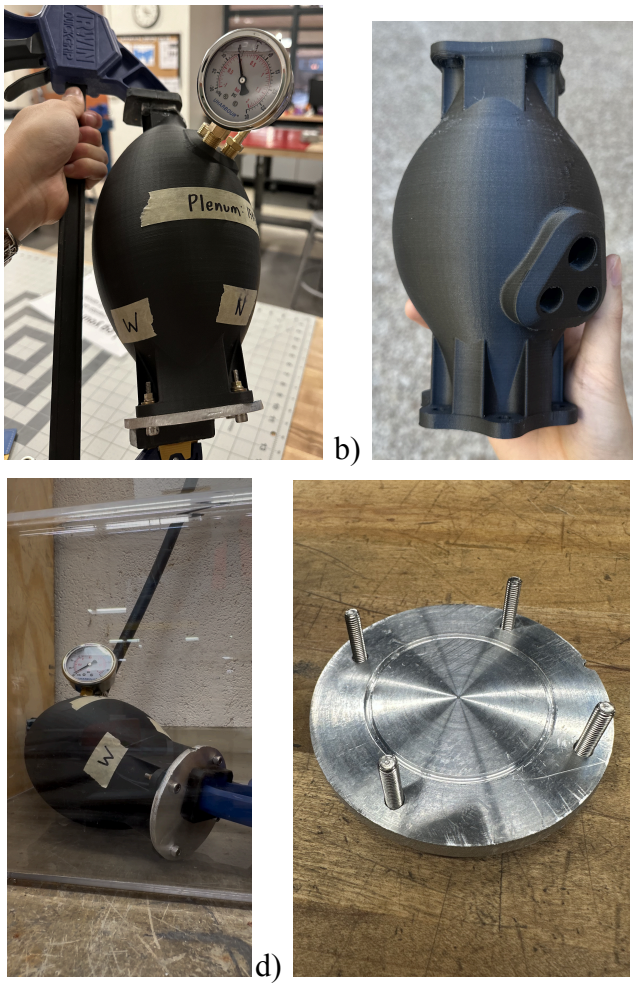

Figure A10. a) 1545 cc Plenum printed in CF-ABS, sealed and fitted with a barb and vacuum gauge. The top is sealed with epoxy. The bottom is sealed with an O-ring/gasket. b) 753 cc Plenum, printed in CF-ASA c) Plenum holding 30 inHg vacuum. Black line connected to vacuum pump. d) Bottom face plate, with an O-ring groove.

Figure A11. Leak test with O-ring. Air shown leaking from layer lines and bottom interface.

a) 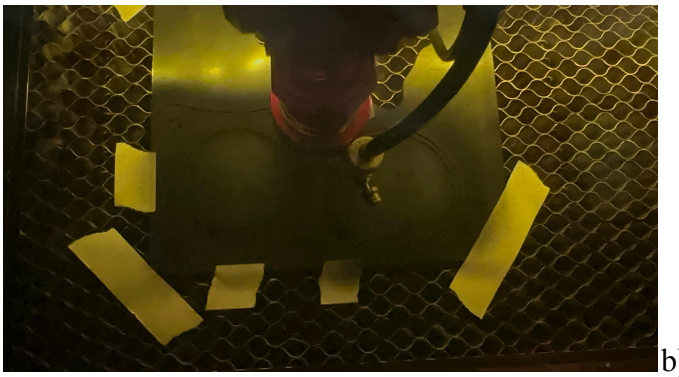 b) 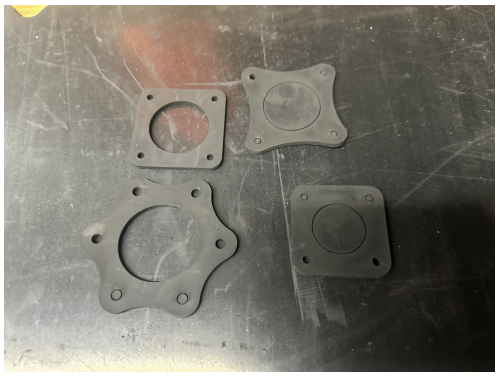

Figure A12. Gaskets. a) Gaskets being laser cut. b) Completed gaskets, before being washed.